RSC Advances

ROYAL SOCIETY OF CHEMISTRY

www.rsc.org/advances

RSC Advances

ARTICLE

Synthesis and characterisation of permethylindenyl zirconium complexes and their use in ethylene polymerisation

Received 00th January 20xx,
Accepted 00th January 20xx

DOI: 10.1039/x0xx00000x

www.rsc.org/

Jean-Charles Buffet, Thomas A. Q. Arnold, Zoë R. Turner, Phakpoom Angpanitcharoen, and Dermot O'Hare*

We report the synthesis of two zirconocenes, dimethylsilylbis(hexamethylindenyl) zirconium dichloride, *rac*-(SBI*)$ZrCl_2$ and ^{n}butyldimethylsilyl(hexamethylindenyl) zirconium trichloride $[(Ind^*SiMe_2{}^nBu)Zr(\mu\text{-}Cl)Cl_2]_2$. The complexes were characterised by NMR spectroscopy and X-ray crystallography, and the bonding was evaluated using density functional theory. *rac*-(SBI*)$ZrCl_2$ demonstrated a very high activity for solution phase polymerisation of ethylene (*ca.* 22500 $kg_{PE}/mol_{Zr}/h/bar$). Both *rac*-(SBI*)$ZrCl_2$ and *rac*-(EBI*)$ZrCl_2$ (EBI* = ethylenebis(hexamethylindenyl) have been supported on MAO modified silica and AMOST layered double hydroxides (AMO-LDHs), and evaluated as catalysts in the slurry-phase polymerisation of ethylene. The highest catalytic polymerisation activities for *rac*-(SBI*)$ZrCl_2$ and *rac*-(EBI*)$ZrCl_2$ on the layered double hydroxides were 9657 and 4325 $kg_{PE}/mol_{Zr}/h/bar$ respectively for MAO modified $Mg_2Al\text{-}SO_4$ LDH. However, *rac*-(EBI*)$ZrCl_2$ was a three times more active catalyst than *rac*-(SBI*)$ZrCl_2$ when supported on silica.

Introduction

Well-defined group 4 metallocenes have offered an important alternative technology to the ethylene polymerisation field dominated by Ziegler-Natta and Philips catalysts.[1,2] In contrast to the heterogeneous Ziegler-Natta systems, metallocene catalysts produce polyethylene with narrow molecular weight distributions and polydispersity indices close to two. Furthermore, the single-site nature of their active sites enables the polymer properties to be fine-tuned.[3]

Studies of bridged metallocene compounds have shown that slight variations of the ring substituents and bridging groups can massively influence the activity of ethylene polymerisation.[4,5] The electronic structure and spatial organisation of the active site of the catalyst, influenced by ligand structure, have profound effects on the microstructure of the polyethylene obtained and hence, the overall polymer properties.[6,7]

Support materials provide a convenient way to serve as a template for the growing polymer particle.[8] Many materials have been tested as polymerisation supports including inorganic solids such as clays,[9] ZrO_2,[10] SiO_2,[11] and $MgCl_2$.[2] Silica (SiO_2) is the most commonly used support for immobilising metallocene complexes.[11] Modified silicas, such as mesoporous SBA-15,[12,13] MCM-41,[14,15] and nanostructured silica materials,[16,17] have also been investigated. Layered double hydroxide (LDHs) are a class of hydrotalcite-like clays containing positively charged layers with intercalated anions between them.[18-24] It is most typical for the metal ions to be divalent and trivalent. The common divalent metal ions include Mg^{2+} and Ca^{2+}, while the trivalent metal ion is typically Al^{3+}. The intercalated anions show more variety, and while they can include large anionic organic salts, they are more typically inorganics such as CO_3^{2-}, SO_4^{2-} or Cl^-. Recently, we developed a new generation of LDHs using an aqueous miscible solvent treatment (AMOST) method.[19-21] The AMO-LDHs made in this way exhibit surface areas two orders of magnitude in excess of those previously reported (*ca.* 400 m^2/g). We showed via an EXAFS study that they are well-ordered supports for slurry phase polymerisation of ethylene.[22-23]

We report here the synthesis and characterisation of two new permethylated indenyl zirconium complexes, their reaction with both a MAO-treated layered double hydroxide and silica to form supported catalyst systems and their use in the slurry and solution polymerisation of ethylene.

Results and discussion

Synthesis of pro-ligands

The synthesis of the dimethylsilylbis(hexamethylindene) (SBI*)H_2 ligand was previously reported by O'Hare and co-workers but the compound was not crystallographically characterised.[24]

Chemistry Research Laboratory, Department of Chemistry, University of Oxford, 12 Mansfield Road, OX1 3TA, Oxford, UK. E-mail: dermot.ohare@chem.ox.ac.uk, Tel: +44 (0) 1865 272686.

Electronic Supplementary Information (ESI) available: [General details, NMR spectroscopy, X-ray crystallography, computational details and definitions of structural parameters]. See DOI: 10.1039/x0xx00000x

Single crystals of *rac*-(SBI*)H_2 suitable for an X-ray diffraction study were obtained from a saturated hexane solution at room temperature. The molecular structure of (SBI*)H_2 is shown in Fig. 1. Selected bond lengths and angles are given in Table S1. The stereochemistry of the two chiral centres and the space group ($P\bar{1}$) show that the crystal corresponds to a racemic mixture of *rac*-(SBI*)H_2.

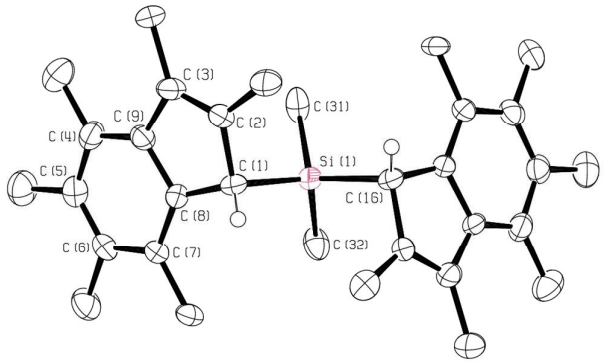

Fig. 1 Molecular structure of (*S*,*S*)-*rac*-(SBI*)H_2. Ellipsoids are drawn at 50% probability level. Hydrogen atoms, except for at the chiral centres, are omitted for clarity.

Reaction of one equivalent of (SBI*)H_2 with two equivalents of ^{n}butyllithium in thf for 16 h afforded lithium dimethylsilylbis(hexamethylindenide), (SBI*)Li_2 as yellow powder in quantitative yield.[24]

However, when the reaction was carried out in a pseudo one-pot starting from the hexamethylindene and with a shortened reaction time of 2 h (from 16 h), Lithium ^{n}butyldimethylsilyl(hexamethylindenide), LiInd*SiMe$_2{}^n$Bu, was afforded as a colourless solid in 83% yield, Scheme 1.

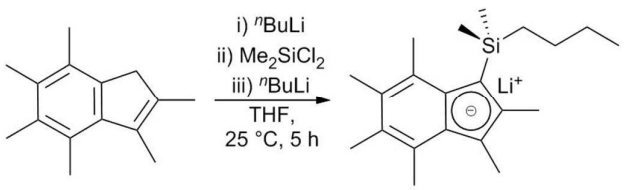

Scheme 1 Synthesis of lithium ^{n}butyldimethylsilyl(hexamethylindenide) (LiInd*SiMe$_2{}^n$Bu).

The ^{1}H NMR spectrum of LiInd*SiMe$_2{}^n$Bu in pyridine-d_5 (Figure S5) shows six singlets corresponding to the ring methyl groups at approximately 2.4-3.1 ppm and a singlet at 0.73 ppm, with intensity six, is attributed to the silicon methyl groups. A triplet at 0.92 ppm corresponds to the butyl terminal CH_3, while the three multiplets at 1.27, 1.47 and 1.72 ppm represent the methylene groups α, γ and β to the silicon respectively.

Synthesis of complexes

Stoichiometric reaction of (SBI*)Li_2 and $ZrCl_4$ in benzene at room temperature led to the formation of *rac*-(SBI*)$ZrCl_2$ as an orange crystalline material in 34% yield (Scheme 2). No evidence of *meso*-(SBI*)$ZrCl_2$ was seen in any reaction aliquots analysed by ^{1}H NMR spectroscopy – a marked change from the previous syntheses of (EBI*)$ZrCl_2$ and (SBI*)Fe where 50:50 *rac*-:*meso*- isomeric mixtures were obtained.[7,24] Reactions in toluene or thf led to yields below 10%.

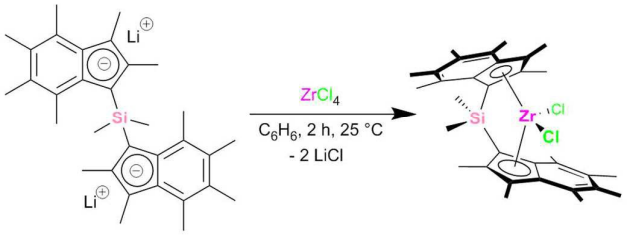

Scheme 2 Synthetic pathway to *rac*-(SBI*)$ZrCl_2$

Single crystals suitable for an X-ray crystallographic study were grown from a benzene solution at room temperature. The molecular structure is represented in Fig. 2. Selected bond lengths and angles are given in Table S3.

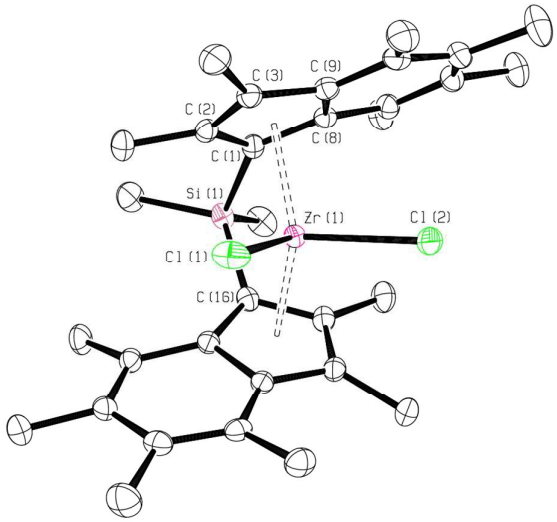

Fig. 2 Molecular structure of *rac*-(SBI*)$ZrCl_2$. Hydrogen atoms are omitted for clarity. Thermal ellipsoids drawn at 50%.

rac-(SBI*)$ZrCl_2$ crystallises in the monoclinic spacegroup $P2_1/n$, with one molecule in the asymmetric unit and four molecules in the unit cell – two of each enantiomer. The first point of note is that the value of torsion angle, TA'‡ (145.15°) is larger than 90° showing that the two indenyl rings are pointed in opposite directions as is expected for a *rac*-isomer. This value of TA'‡ agrees well with that reported for *rac*-(SBI)$ZrCl_2$, 145.20°,[25] and implies that the constraints of the dimethylsilicon bridge outweigh any steric effects from the permethylation. The tilt angle, α‡, (58.50°), is slightly lower than that reported for either (SBI)$ZrCl_2$ (61.80°) or ($^{2,4,6\text{-}Me_3}$SBI)$ZrCl_2$ (59.18°).[26] The value of α is also in good agreement with that of *rac*-(EBI*)$ZrCl_2$ (57.15°),[7] This β‡ value for *rac*-(SBI*)$ZrCl_2$ (18.89°), slightly exceeds those reported for ($^{2,4,6\text{-}Me_3}$SBI)$ZrCl_2$ (17.05°) or (SBI)$ZrCl_2$ (16.45°).[27] The average Zr-Cp_{cent} distance (2.251 Å) fits well with other values reported in the literature for *ansa*-bridged species including (EBI*)$ZrCl_2$ (2.240 Å), (SBI)$ZrCl_2$ (2.241 Å) and ($^{2,4,6\text{-}Me_3}$SBI)$ZrCl_2$ (2.231 Å),

and also with unbridged examples such as $(Ind^*_2)ZrCl_2$ (2.257 Å) and $(Ind_2)ZrCl_2$ (2.231 Å).[8,27]

Geometry optimisation calculations were performed at the B3LYP[28,30] and BP86[31,32] level of DFT with those using the BP86 functional most successfully reproducing the established experimental metrical parameters of *rac*-(SBI*)$ZrCl_2$; slightly increased rotation and larger tilt angles were observed. (Table 1).

Table 1 Comparison of selected experimental and calculated bond lengths (Å), angles (°) and geometric parameters (°) of *rac*-(SBI*)$ZrCl_2$.

	Experimental	Calculated B3LYP	Calculated BP86
Avg. Zr-Cp_{cent}	2.251	2.308	2.288
Avg. Zr-Cl	2.423	2.442	2.428
C(1)-Si(1)-C(16)	96.22(7)	96.31	95.85
α	58.50	61.28	59.95
TA'	145.15	148.44	146.30

Illustrations of the DFT-computed (BP86) HOMO and LUMO are given in Fig. 3. The HOMO primarily consists of ligand p-orbitals; localised double bond character within the benzene rings is implied. In contrast, the LUMO is primarily based on the d^0 metal centre (29.0% Zr d_{xy} orbital component).

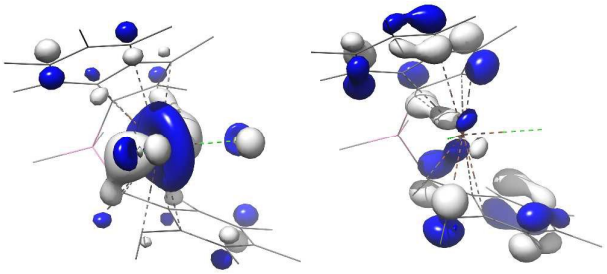

Fig. 3 Illustration of the DFT-computed LUMO (left) and HOMO (right) of *rac*-(SBI*)$ZrCl_2$ at the BP86 level of theory.

The ^{1}H NMR spectrum of *rac*-(SBI*)$ZrCl_2$ in chloroform-d_1 shows six singlets between 1.25 and 2.50 ppm. There is one resonance for the two silyl methyl groups which are in the same environment in solution and at low frequency (1.34 ppm).

Stoichiometric reaction of LiInd*$SiMe_2{}^n$Bu with $ZrCl_4$ in toluene for two hours led to $[(Ind^*SiMe_2{}^nBu)Zr(\mu\text{-}Cl)Cl_2]_2$ as a red crystalline solid in 73% yield (Scheme 3).

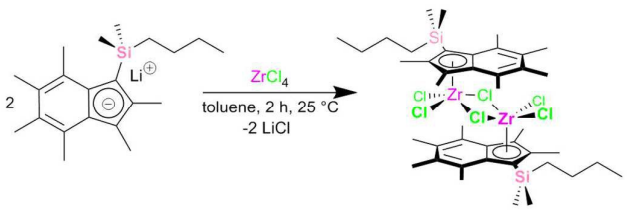

Scheme 3 Synthesis of ^{n}butyldimethylsilyl(hexamethylindenyl) zirconium trichloride $[(Ind^*SiMe_2{}^nBu)Zr(\mu\text{-}Cl)Cl_2]_2$.

The crystalline material was found to be suitable for analysis by X-ray diffraction, the molecular structure of $[(Ind^*SiMe_2{}^nBu)Zr(\mu\text{-}Cl)Cl_2]_2$ is depicted in Fig. 4.

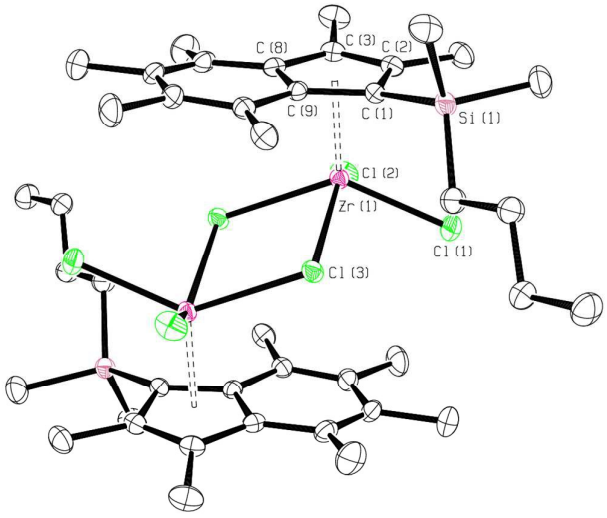

Fig. 4 Molecular structure of $[(Ind^*SiMe_2{}^nBu)Zr(\mu\text{-}Cl)Cl_2]_2$. Hydrogens omitted for clarity. Thermal ellipsoids drawn at 50%.

$[(Ind^*SiMe_2{}^nBu)Zr(\mu\text{-}Cl)Cl_2]_2$ crystallises in the triclinic spacegroup $P\bar{1}$, with half a dimer in the asymmetric unit (Fig. 4). The Zr(1)-Cp_{cent} distance (2.190 Å) is comparable to that in polymeric $CpZrCl_3$ which has Zr-Cp_{cent} distances of 2.196 Å.[33] The bond lengths for the terminal chlorides (2.4037(4) and 2.3982(4) Å) are significantly shorter than those of the bridging chlorides (2.5837(4) Å). These agree well with the Zr-Cl distances reported for $[CpZrCl_3]_n$ of 2.419(3) Å for the terminal chloride and 2.518(3) and 2.728(3) Å for the bridging ligands.

DFT calculations were performed on $[(Ind^*SiMe_2{}^nBu)Zr(\mu\text{-}Cl)Cl_2]_2$ and highlight the localised double bonds in the benzene rings in the HOMO. The LUMO is again primarily Zr-based with a 27.3% d_{xy} orbital component on each metal centre. (Figure 5 and Table 2).

$[(Ind^*SiMe_2{}^nBu)Zr(\mu\text{-}Cl)Cl_2]_2$ was analysed by ^{1}H NMR spectroscopy in benzene-d_6, Figure S7, six singlets representing the indenyl methyl groups appear in the range 1.96-2.57 ppm and there are two singlets at 0.55 and 0.65 ppm corresponding to the silyl methyl groups. Multiplets relating to the butyl substituent appear at 0.86, 1.00, 1.26 and 1.29 ppm for the δ, α, γ and β positions respectively.

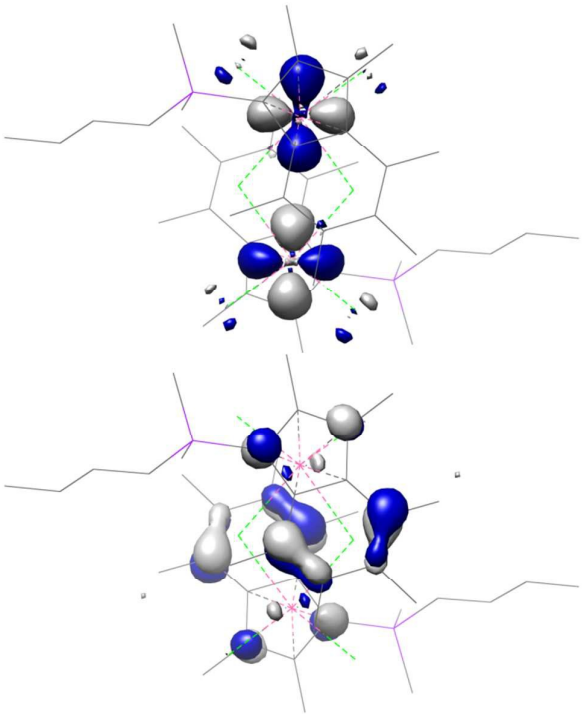

Fig. 5 Illustration of the DFT-computed LUMO (top) and HOMO (bottom) of $[(Ind^*SiMe_2{}^nBu)Zr(\mu\text{-}Cl)Cl_2]_2$ at the BP86 level of theory.

Table 2 Comparison of selected experimental and calculated bond lengths (Å), angles (°) and geometric parameters (°) of $[(Ind^*SiMe_2{}^nBu)Zr(\mu\text{-}Cl)Cl_2]_2$.

	Experimental	Calculated B3LYP	Calculated BP86
Zr-Cp_{cent}	2.190	2.234	2.215
Avg. Zr-$Cl_{terminal}$	2.4011	2.420	2.418
Avg. Zr-$Cl_{bridging}$	2.5835	2.656	2.643
Cl(1)-Zr(1)-Cl(2)	91.233(17)	90.74	91.59

Synthesis of solid ethylene polymerisation pre-catalysts

We have investigated the use of two different catalyst supports: silica and AMO-LDH due to their proven excellent activities in the literature.[22,23,34,35] Both support materials were calcined before use: SiO_2 at 600 °C for two hours under a flow of N_2 and AMO-LDH at 150 °C for six hours under high vacuum (2×10^{-2} mbar). The surface of both supports was then treated with 0.5 equivalents of MAO; producing MAO modified silica (SSMAO) and MAO modified AMO-LDH (LDHMAO) with a maximum loading of 15 and 13.5 wt% aluminium (from methylaluminoxane) in the resulting SSMAO and LDHMAO respectively. Immobilisation of the complex was achieved by addition of toluene to a mixture of the complex and MAO-activated support, followed by heating at 60 °C for one hour. After work-up, all the solids were afforded as coloured powders in good yield (>80%).

Scanning electron microscopy (SEM) images for the silica immobilisation illustrates an uniform shape and size distribution, Fig. S10. The particles are not spherical but granular with an average size of approximately 10 µm. They do not change in either shape or dimension on reaction with MAO, nor on the immobilisation of *rac*-(SBI*)$ZrCl_2$.

SEM-EDX analysis demonstrated the desired elements on the surface (C, 14.3; Al, 2.6; O, 62.9; Si, 19.4 (%)) (Fig. S10).

^{13}C CPMAS NMR spectroscopy was used to characterise LDHMAO-(SBI*)$ZrCl_2$ (Fig. S8). The dominant resonance at −9 ppm corresponds to the highly shielded methyl environment of MAO. Resonances between 22 and 34 ppm correspond to the methyl groups around the rings of *rac*-(SBI*)$ZrCl_2$ while a slightly weaker resonance is also observed at 13 ppm which corresponds to the low frequency silicon methyl groups. The ^{29}Si CPMAS NMR spectrum shows a single silicon environment found for the SiO_2 within SSMAO was observed at −105 ppm; the resonance for the silyl methyl group in the ligand was too weak to be identified (Fig. S9).

Solution phase polymerisation of ethylene

The solution phase polymerisations were all carried out under ethylene at a pressure of two bar, with 50 mL hexanes, 0.2 mg of *rac*-(SBI*)$ZrCl_2$ and with an Al:Zr ratio (MAO:*rac*-(SBI*)$ZrCl_2$) of 2000:1. All polymerisation runs were carried out for 30 minutes, or until the stirring of the vessel ceased entirely. Complete polymerisation data is reported in Tables S7 and S8.

rac-(SBI*)$ZrCl_2$ was used to catalyse the polymerisation of ethylene at a range of temperatures from 40-90 °C using methylaluminoxane (MAO) as the co-catalyst and scavenger (Fig. 6).

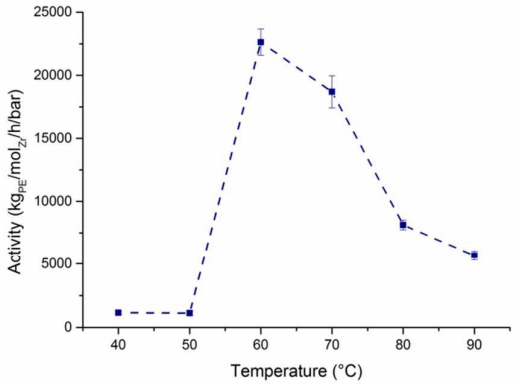

Fig. 6 Solution phase ethylene polymerisation activity dependence of *rac*-(SBI*)$ZrCl_2$ on temperature. MAO (2000:1); 2 bar ethylene; 0.2 mg complex loading; 50 mL hexanes; timed until cessation of stirring.

The activity achieved at 60 °C (22 622 $kg_{PE}/mol_{Zr}/h/bar$) compares well with some of the highest reported values in the literature; *rac*-(EBI*)$ZrCl_2$ (61 800 $kg_{PE}/mol_{Zr}/h/bar$, 70 °C);[7] *rac*-(SBI)$ZrCl_2$, *rac*-($^{2,4,6\text{-}Me_3}$SBI)$ZrCl_2$ and Cp_2ZrCl_2 (18 450, 44 760 and 30 450 $kg_{PE}/mol_{Zr}/h/bar$ respectively, 30 °C).[36,37] There is a sharp increase in activity seen between 50 and 60 °C (1 123 and 22 622 $kg_{PE}/mol_{Zr}/h/bar$ respectively). Similar features were reported by Eskelinen *et al*. who attributed a sharp rise in activity between 70 and 80 °C to an increase in the solubility of the PE chain (in *n*-heptane), allowing for better monomer diffusion to the catalytic centre.[38] A marked decline

in activity is also noted between 70 and 80 °C (18 703 and 8130 $kg_{PE}/mol_{Zr}/h/bar$), suggesting decomposition at elevated temperatures.[39] These values are much higher than the recently reported bis(pentamethyl)zirconium dichloride complexes (activity around 400 $kg_{PE}/mol_{Zr}/h/bar$).[40] The weight average molecular weights, M_w, were high (213 927 and 261 337 $kg.mol^{-1}$ 60 and 70 °C respectively).

A study was undertaken at 70 °C with *rac*-(SBI*)$ZrCl_2$ to test the effect that the Al:Zr ratio has on activity (Fig. 7).

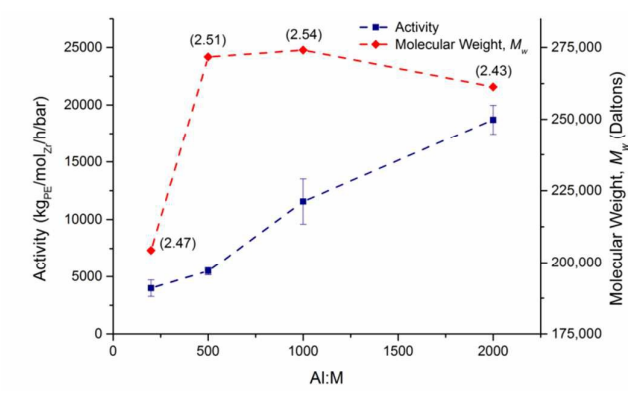

Fig. 7 Dependence of solution phase ethylene polymerisation activity and molecular weight, M_w, for *rac*-(SBI*)$ZrCl_2$ on the Al:Zr co-catalyst (MAO) ratio. PDIs are given in parentheses. 70 °C; 2 bar ethylene; 0.2 mg catalyst loading; 50 mL hexanes; timed until cessation of stirring.

The activity at 2000:1 is more than four times greater than that at 200:1 (18 703 and 3996 $kg_{PE}/mol_{Zr}/h/bar$ respectively). At an Al:Zr ratio of 200:1, M_w was 204 374 $kg.mol^{-1}$ rising quickly to 271 713 $kg.mol^{-1}$ at a ratio of 500 and plateauing on further increases. This contrasts with reports in the literature that suggest that M_w will decrease on addition of more MAO,[41] or at the very least remain constant.[42] Attempts were also made, not only to vary the Al:Zr ratio, but to vary the source of aluminium. Polymerisation attempts with 2000 equivalents of Al^iBu_3 (TIBA) and $AlMe_3$ (TMA) failed to produce any polyethylene.

Table 3 Comparison of selected solution phase polymerisation data.

	Activity ($kg_{PE}/mol_{Zr}/h/bar$)	M_w (g/mol)	M_w/M_n	*Ref*
rac-(SBI*)$ZrCl_2$	22622	213927	2.32	This[a]
rac-(EBI*)$ZrCl_2$	61800	215000	2.40	7[b]
rac-(SBI)$ZrCl_2$	18450	260000	2.30	37[c]
rac-($^{2,4,6\text{-}Me3}$SBI)$ZrCl_2$	44760	250000	-	36[c]
Cp_2ZrCl_2	30450	62000	2.00	37[c]
rac-(Ind[#])$ZrCl_2$	433	313893	3.07	40[d]

[a]60 °C, 2 bar ethylene, 50 mL hexanes. [b]70 °C, 10 bar ethylene, 1.8 L isobutene. [c]30 °C, 2 bar ethylene, 5 mL toluene. [d]30 °C, 2 bar ethylene, 5 mL toluene

Slurry phase polymerisation of ethylene

Slurry phase polymerisations of ethylene were carried out using methylaluminoxane derived silica (SSMAO) and AMO-LDHs (LDHMAO) supported permethylindenyl catalysts. The slurry phase polymerisations were carried out similarly to the solution phase polymerisation with 10 mg of pre-catalysts. No leaching occurred during the slurry phase polymerisation. Complete polymerisation data is reported in Tables S9-S11.

We previously reported the solution phase polymerisation of ethylene using *rac*-(EBI*)$ZrCl_2$ but no slurry polymerisation were carried out.[7] Figs. 8 and 9 depict the ethylene polymerisation activity and the molecular weight data for SSMAO/ *rac*-(EBI*)$ZrCl_2$. The activities have an optimum (2151 $kg_{PE}/mol_{Zr}/h/bar$ at 60 °C) and are comparatively stable (i.e. above 1500 $kg_{PE}/mol_{Zr}/h/bar$) from 50-80 °C, higher than the reported results for $(Ind)_2ZrCl_2$ supported on silica with trimethylalumnium (400 $kg_{PE}/mol_{Zr}/h/bar$).[43]

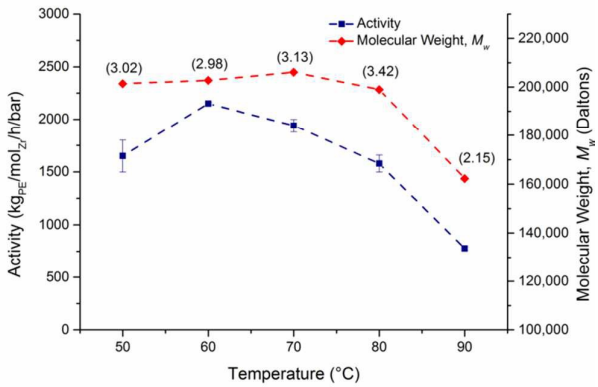

Fig. 8 Dependence of slurry phase ethylene polymerisation activity and M_w for *rac*-(EBI*)$ZrCl_2$ on temperature. PDIs are given in parentheses. Supported on SSMAO (200:1 loading); TIBA co-catalyst; 2 bar ethylene; 10 mg catalyst; 50 mL hexanes; 1 hour.

The molecular weight observed in the temperature range 50-80 °C is remarkably constant at just over 200 000 $kg.mol^{-1}$ before dropping off to 162 273 $kg.mol^{-1}$ at 90 °C.

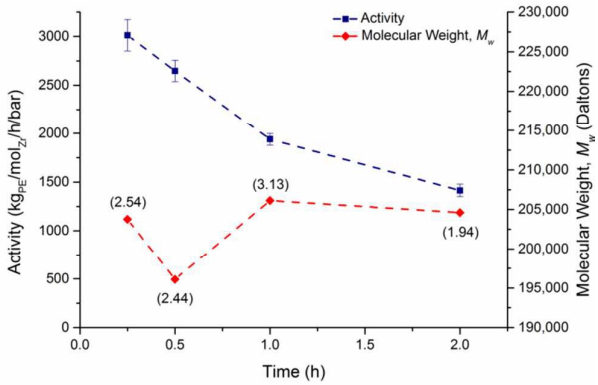

Fig. 9 Dependence of slurry phase ethylene polymerisation activity and molecular weight, M_w, for *rac*-(EBI*)$ZrCl_2$ on length of run. PDIs are given in parentheses. Supported on SSMAO (200:1 loading); TIBA co-catalyst; 70 °C; 2 bar ethylene; 10 mg catalyst; 50 mL hexanes.

The activities decreased with increasing time of polymerisation (3012 to 1414 $kg_{PE}/mol_{Zr}/h/bar$ for 15 minutes to two hours), consistent with literature reports.[41]

Data for the slurry phase polymerisation of ethylene using SSMAO/ *rac*-(SBI*)$ZrCl_2$ are depicted in Figs. 10 and 11.

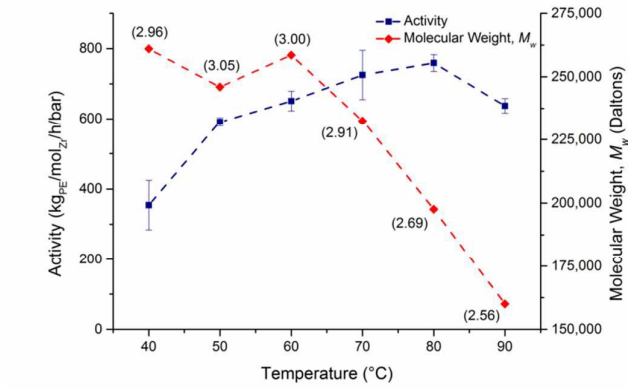

Fig. 10 Dependence of slurry phase ethylene polymerisation activity and M_w for *rac*-(SBI*)$ZrCl_2$ on temperature. PDIs are given in parentheses. Supported on SSMAO (200:1 loading); TIBA co-catalyst; 2 bar ethylene; 10 mg catalyst; 50 mL hexanes; 30 minutes.

The activities increase from 340 to up to 725 $kg_{PE}/mol_{Zr}/h/bar$ (40 to 80 °C respectively). However, as expected the molecular weight decreased with increasing temperature (around 261002 to 160049 $kg.mol^{-1}$).

A comparison of two different loadings of *rac*-(SBI*)$ZrCl_2$ on SSMAO led to the observation of the opposite trend seen for *rac*-(EBI*)$ZrCl_2$. The activities obtained were lower on decreased loading at 70 °C: 725 and 611 $kg_{PE}/mol_{Zr}/h/bar$ (200:1 and 300:1 respectively).

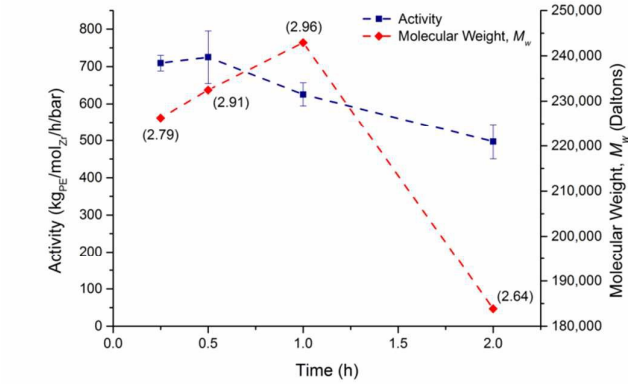

Fig. 11 Dependence of slurry phase ethylene polymerisation activity and M_w for *rac*-(SBI*)$ZrCl_2$ on length of run. PDIs are given in parentheses. Supported on SSMAO (200:1 loading); TIBA co-catalyst; 70 °C; 2 bar ethylene; 10 mg catalyst; 50 mL hexanes.

These results confirmed the findings in solution phase were the ethylene bridge complex was faster the silyl bridge. However, the molecular weights were higher and the polydispersities lower for silyl based systems.

The permethylindenyl complexes *rac*-(EBI*)$ZrCl_2$ and *rac*-(SBI*)$ZrCl_2$ were also supported on an MAO-modified AMOST layered double hydroxides (AMO-LDH)[21-23] and their polymerisation was carried out in similar conditions as the silica supported (Fig. 12).

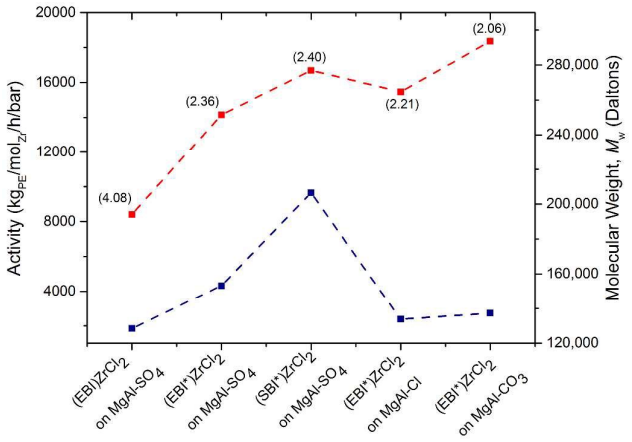

Fig. 12 Dependence of slurry phase ethylene polymerisation activity and M_w for *rac*-(EBI*)$ZrCl_2$ and *rac*-(SBI*)$ZrCl_2$ on various support. PDIs are given in parentheses. Supported on LDHMAO (200:1 loading); TIBA co-catalyst; 2 bar ethylene; 10 mg catalyst; 50 mL hexanes; 60 minutes.

rac-(SBI*)$ZrCl_2$ demonstrated higher activity that its ethylene bridged analogue (*rac*-(EBI*)$ZrCl_2$) and also *rac*-(EBI)$ZrCl_2$) with activities of 9657, 4325 and 1841 $kg_{PE}/mol_{Zr}/h/bar$ respectively. When the LDH support was varied, the catalyst based on Mg_2Al-SO_4 led to the highest activity, followed by Mg_2Al-CO_3 and Mg_2Al-Cl with activities of 9657, 2719 and 2373 $kg_{PE}/mol_{Zr}/h/bar$ respectively. These data corroborate well with our recent studies.[21-22] There is a decrease in the polydispersity when using the permethylindenyl in comparison to the perhydroindenyl complex.

Conclusions

We have reported the synthesis and characterisation by X-ray crystallography and NMR spectroscopy of two new permethylindenyl complexes, *rac*-(SBI*)$ZrCl_2$ and $[(Ind*SiMe_2{}^nBu)Zr(\mu\text{-}Cl)Cl_2]_2$.

rac-(SBI*)$ZrCl_2$ demonstrated very high activity for the solution phase polymerisation (*ca*. 22 500 $kg_{PE}/mol_{Zr}/h/bar$). However, the ethylene analogous compound demonstrated more than double this activity.[7]

MAO-modified AMOST layered double hydroxides support led to higher activity with respect to silica supported pre-catalysts. *rac*-(EBI*)$ZrCl_2$ supported on the AMO-LDH Mg_2Al-SO_4, Mg_2Al-CO_3 and Mg_2Al-Cl displayed polymerisation activities of 4325 2719 and 2373 $kg_{PE}/mol_{Zr}/h/bar$ respectively. *rac*-(SBI*)$ZrCl_2$ supported on the MAO-modified AMO-LDH Mg_2Al-SO_4 was the most active solid catalyst system at 9657 $kg_{PE}/mol_{Zr}/h/bar$.

However, *rac*-(EBI*)$ZrCl_2$ was three times faster than *rac*-(SBI*)$ZrCl_2$ when supported on silica.

Experimental details

Synthesis of LiInd*SiMe$_2{}^n$Bu. 2.00 g of hexamethylindene (10 mmol, 1 eq.) was dissolved in thf (50 mL) and ^{n}BuLi (2.5 M in hexanes; 4.4 mL, 11 mmol, 1.1 eq.) was added dropwise at room temperature, effecting a change in colour to pale pink.

After 2 h, Me_2SiCl_2 (0.64 g, 0.60 mL, 5 mmol, 0.5 eq.) was added causing a slight decolouration in the solution to pale yellow. After 1 h, ^{n}BuLi (2.5 M in hexanes; 4.4 mL, 11 mmol, 1.1 eq.) was added to the reaction mixture and, following stirring at room temperature for 3 h, the reaction was dried under vacuum and the LiInd*SiMe$_2$^{n}Bu was obtained as an off white solid in an 83% yield (1.33 g, 4.15 mmol). ^{1}H NMR (300 MHz, 298 K, pyridine-d_5): δ 0.73 (s, 6H, $SiMe_2$), 0.92 (t, 3H, $^3J_{HH}$ = 7.0 Hz, δ-Bu), 1.27 (m, 2H, α-Bu), 1.48 (m, 2H, γ-Bu), 1.72 (m, 2H, β-Bu), 2.47 (s, 3H, Ar-Me), 2.29 (s, 3H, Ar-Me), 2.82 (s, 3H, Cp-Me), 2.97 (s, 3H, Ar-Me), 3.03 (s, 3H, Cp-Me), 3.05 (s, 3H, Ar-Me). ^{13}C{^{1}H} NMR (75 MHz, 298 K, pyridine-d_5): δ 5.96 ($SiMe_2$), 14.84 (δ-Bu), 16.78 (Me), 17.33 (Me), 17.99 (Me), 18.33 (Me), 18.69 (Me), 23.11 (Me), 23.30 (α-Bu), 28.04 (γ-Bu), 28.77 (β-Bu), 90.71 (C-Si), 105.11 (Cp), 119.02 (Ar), 119.48 (Ar), 122.49 (Ar), 122.97 (Ar), 132.30 (Ar), 135.69 (Cp), 138.02 (Ar). ^{7}Li NMR (156 MHz, 298 K, pyridine-d_5): δ 1.54.

Synthesis of *rac*-(SBI*)ZrCl$_2$. Benzene (50 mL) was added to a mixture of (SBI*)Li_2 (2.00 g, 4.27 mmol) and $ZrCl_4$ (0.98 g, 2.47 mmol) and the reaction mixture was stirred at room temperature for 2 h. The resultant red solution was filtered away from the LiCl by-product, concentrated in vacuum by half and left overnight at room temperature to yield orange crystals. The crystals isolated by filtration and dried to afford orange crystalline material in 34% yield (0.89 g, 1.45 mmol). ^{1}H NMR (400 MHz, 298 K, chloroform-d_1): δ 1.34 (s, 6H, $SiMe_2$), 1.88 (s, 6H, Cp-Me), 2.18 (s, 6H, Ar-Me), 2.30 (s, 6H, Ar-Me), 2.39 (s, 6H, Cp-Me), 2.45 (s, 12H, Ar-Me). ^{13}C{^{1}H} NMR (100 MHz, 298 K, chloroform-d_1): δ 10.94 ($SiMe_2$), 15.93 (Ar-Me), 16.09 (Ar-Me), 16.50 (Ar-Me), 17.52 (Cp-Me), 17.71 (Ar-Me), 22.12 (Cp-Me), 78.02 (Cp-Si), 127.81 (Me), 129.90 (Me), 130.17 (Me), 130.35 (Me), 130.89 (Me), 133.17 (Me), 134.31 (Me), 135.40 (Me). IR (KBr) (cm^{-1}): 2961, 2923, 1543, 1454, 1384, 1260, 1097, 1020, 850, 813, 668. MS (EI): found 615.7972; calculated 615.7908. Major fragmentation peaks noted for M−Me (600.78).

Synthesis of [(Ind*SiMe$_2$^{n}Bu)Zr(μ-Cl)Cl$_2$]$_2$. To a mixture of LiInd*SiMe$_2$^{n}Bu (1.00 g, 3.12 mmol, 1 eq.) and $ZrCl_4$ (0.72 g, 3.12 mmol, 1 eq.) was added toluene (50 mL). This resulted in a bright orange slurry which became vermillion in colour on stirring for a further 2 h. The slurry was allowed to settle and the supernatant was filtered off and left to stand at −35 °C for three days affording [(Ind*SiMe$_2$^{n}Bu)Zr(μ-Cl)Cl$_2$]$_2$ as a red crystalline solid suitable for an X-ray diffraction study in 73% yield (1.16 g, 2.28 mmol). ^{1}H NMR (400 MHz, 298 K, benzene-d_6)**:** δ 0.55 (s, 3H, Si-Me$_2$), 0.65 (s, 3H, Si-Me$_2$), 0.86 (t, ^{3}J$_{HH}$ = 7.0 Hz, 3H, δ-Bu), 1.01 (m, 2H, α-Bu), 1.25 (m, 2H, β-Bu), 1.29 (m, 2H, γ-Bu), 1.96 (s, 3H, Ar-Me), 2.03 (s, 3H, Ar-Me), 2.31 (s, 3H, Cp-Me), 2.42 (s, 3H, Ar-Me), 2.48 (s, 3H, Cp-Me), 2.57 (s, 3H, Ar-Me). ^{13}C{^{1}H} NMR (100 MHz, benzene-d_6): δ 3.37 (Si-Me$_2$), 3.75 (Si-Me$_2$), 13.98 (δ-Bu), 15.92 (Cp-Me), 16.78 (Ar-Me), 17.31 (Ar-Me), 17.31 (Ar-Me), 17.87 (Cp-Me), 19.79 (α-Bu), 21.71 (Ar-Me), 26.82 (γ-Bu), 26.89 (β-Bu), 116.31 (Cp), 126.23 (Cp), 130.46 (Ar), 132.48 (Ar), 133.23 (Ar), 134.05 (Ar), 136.57 (Ar), 137.24 (Ar), 143.54 (Cp). IR (KBr) (cm^{-1}): 3573, 2957, 1457, 1385, 1261, 1217, 1098, 814, 690, 480. HRMS (EI): found 508.0464; calculated 508.0460.

Synthesis of solid polymerisation catalysts. The quantity of catalyst immobilised on the surface of the support is given in terms of the Al:Zr ratio of the methylaluminoxane component to the organometallic complex. In the case of SSMAO and LDHMAO, 0.5 eq. MAO is used to activate the surface of each support. The ratios used in this work are 300:1 and 200:1. The molecular weights used for SiO_2 and LDH ($Mg_{0.75}Al_{0.25}(OH)_2(SO_4)_{0.125}$) are 59.97 and 70.73 kg.mol^{-1} respectively. This gives rise to molecular masses of SSMAO and LDHMAO of 177.94 and 199.46 kg.mol^{-1}. SSMAO and LDHMAO are prepared by weighing out silica or LDH and the MAO into a Schlenk tube in the glovebox and adding toluene to the mixture which is then heated at 60 °C for 1 h with regular swirling, until no further effervescence is observed. The solid is allowed to settle, the solution decanted, and the product dried under vacuum with gentle heating (50 °C) to ensure all the solvent was removed. In the glovebox, the activated support and complex was weighed out into a second Schlenk tube. Toluene (e.g. 50 mL) is added and the reaction mixture swirled swirled at 60 °C for 1 h. The coloured solid is allowed to settle from the clear, colourless solution which is decanted, and the solid is dried *in vacuo* (40 °C, 1 × 10^{-2} mbar).

Solution phase ethylene polymerisation studies. *rac*-(SBI*)$ZrCl_2$, and the methylaluminoxane were charged into an ampoule in a glovebox and 50 mL of hexanes was added. The resulting polyethylene was immediately filtered under vacuum through a dry sintered glass frit. The reactions were performed under 2 bar of ethylene in a 200 mL ampoule, with 0.2 mg of the complex. The reactions were run for 15-120 minutes at varying temperatures. The polyethylene product was then washed with pentane (2 × 5 mL) and then dried on the frit for at least 1 h. The tests were carried out at least twice for each individual set of polymerisation conditions. The activity values were reported as an average with ±1 SD error.

Slurry phase ethylene polymerisation Studies. The silica-supported zirconocene catalysts were tested for their ethylene polymerisation activity under slurry conditions in the presence of tri(isobutyl)aluminium (TIBA), an aluminium-based scavenger. The reactions were performed under 2 bar of ethylene in a 200 mL ampoule, with 10 mg of the catalyst suspended in 50 mL of hexane. The polyethylene work-up was similar to the solution phase polymerisation.

X-ray crystallography. Crystals were mounted on MiTeGen MicroMounts using perfluoropolyether oil, then transferred to a goniometer head on the diffractometer and cooled rapidly to 150 K in a stream of cold nitrogen using an Oxford Cryosystems CRYOSTREAM unit. For *rac*-(SBI*)$ZrCl_2$ and [(Ind*SiMe$_2$^{n}Bu)Zr(μ-Cl)Cl$_2$]$_2$, raw frame data were collected at 150 K using a Enraf-Nonius Kappa CCD diffractometer using graphite monochromated Mo Kα radiation (λ = 0.71073 Å),[44] reduced using DENZO-SMN[45] and corrected for absorption using SORTAV.[46] The structures were solved using direct methods (SHELXS)[47] or a charge-flipping algorithm (SUPERFLIP)[48] and refined by full-matrix least-squares procedures using the Win-GX program suite.[49] The data collection for (SBI*)H_2 was carried out on an Oxford Diffraction Supernova diffractometer using mirror-monochromated Cu *Kα*

radiation (λ = 1.54178 Å) and data were processed using CrysalisPro[50] and refined using full matrix least-squares using CRYSTALS.[51,52]

***rac*-(SBI*)H$_2$**: $C_{32}H_{44}Si$, Triclinic ($P\bar{1}$), a = 9.2291(7) Å, b = 9.7804(7) Å, c = 15.8873(12) Å, α = 89.600(6)°, β = 81.392(6)°, γ = 73.234(6)°, V = 1356.64(18) Å^3, Z = 2, λ = 1.54180 Å, T = 150(2) K, μ = 0.87 mm^{-1}, 5617 independent reflections, Rint = 0.081; R1 = 0.097, wR2 = 0.279. CCDC 1001294.

***rac*-(SBI*)ZrCl$_2$**: $C_{32}H_{42}SiCl_2Zr$, Monoclinic (P21/n), a = 14.1078(1) Å, b = 14.2840(2) Å, c = 14.3753(2) Å, α = γ = 90°, β = 96.8940(5)°, V = 2875.91(6) Å^3, Z = 4, λ = 0.71073 Å, T = 150(2) K, μ = 0.63 mm^{-1}, 6558 independent reflections, Rint = 0.013; R1 = 0.030, wR2 = 0.073. CCDC 1001295.

[(Ind*SiMe$_2$^{n}Bu)Zr(μ-Cl)Cl$_2$]$_2$: $C_{21}H_{33}SiCl_3Zr$, Triclinic, $P\bar{1}$, a = 9.52710(10) Å, b = 11.12740(10) Å, c = 11.36160(10) Å, α = 78.1654(5)°, β = 87.3403(5)°, γ = 77.9022(5)°, V = 1152.67(2) Å^3, Z = 2, λ = 0.71073 Å, T = 150(2) K, μ = 0.88 mm^{-1}, 5248 independent reflections, Rint = 0.013; R1 = 0.030, wR2 = 0.073. CCDC 1419346.

Solid-state NMR spectroscopy data. LDHMAO-*rac*-(SBI*)ZrCl$_2$. ^{13}C CPMAS NMR: δ −9.32 (AlOMe), 12.87 (SiMe2), 22.44 (Ar-Me), 24.57 (Ar-Me), 29.54 (Ar-Me), 31.10 (Ar-Me), 74.97 (Cp), 128.39 (Ar). ^{27}Al CPMAS NMR: δ −527, −28, 470. **SSMAO-EBI*ZrCl2.** ^{13}C CPMAS NMR: δ −9.03 (AlOMe). ^{27}Al CPMAS NMR: δ −309, −113, 3, 182, 336. ^{29}Si CPMAS NMR: δ −106.

Acknowledgements

The authors would like to thank SCG Chemicals Ltd, Thailand for financial support, Dr. Nicholas H. Rees (University of Oxford) for the solid state NMR spectroscopy experiments and Chemical Crystallography (University of Oxford) for the use of the diffractometers. Z.R.T gratefully acknowledges Trinity College, Oxford for a Junior Research Fellowship.

Notes and references

‡ Definitions of the structural parameters (TA, RA, α, β) are detailed in the supporting information.

1 L. Resconi, L. Cavallo, A. Fait and F. Piemontesi, *Chem. Rev.*, 2000, **100**, 1253.
2 G. G. Hlatky, *Chem. Rev.*, 2000, ***100***, 1347.
3 (a) W. Kaminsky, A. Funck and H. Hähnsen, *Dalton Trans.*, 2009, 8803. (b) W. Kaminsky, *Macromol. Chem. Phys.*, 1996, **197**, 3907. (c) H. Sinn, W. Kaminsky, H. J. Vollmer and R. Woldt, *Angew. Chem. Int. Ed.*, 1980, **19**, 390.
4 P. C. Möhring and N. J. Coville, *J. Organomet. Chem.,* 1994, **479**, 1.
5 B. Wang, *Coord. Chem. Rev.*, 2006, **250**, 242.
6 S. Ahmadjo, H. Arabi, M. Nekoomanesh, S. M. M. Mortazavi, G. Zohuri, M. Ahmadi and S. Bolandi, *Chem. Eng. Technol.*, 2011, **34**, 249.
7 P. Ransom, A. E. Ashley, N. D. Brown, A. L. Thompson and D. O'Hare, *Organometallics,* 2011, **30**, 800.
8 R. Duchateau, *Chem. Rev.*, 2002, **102**, 3525.
9 P. A. Zapata, C. Belver, R. Quijada, P. Aranda and E. Ruiz-Hitzky, *Appl. Catal. A: Gen.*, 2013, **453**, 142.
10 T. Pothirat, B. Jongsomjit and P. Praserthdam, *Catal. Commun.,* 2008, **9**, 1426.
11 P. Wongwaiwattanakul and B. Jongsomjit, *Catal. Commun.*, 2008, **10**, 118.
12 D. Bianchini, F. C. Stedile and J. H. Z. dos Santos, *Appl. Catal. A: Gen.*, 2004, **261**, 57.
13 E. Casas, R. van Grieken and J. M. Escola, *Appl. Catal. A: Gen.,* 2012, **437-438**, 44.
14 J. Moreno, R. van Grieken, A. Carrero and B. Paredes, *Macromol. Symp.*, 2011, **302**, 198.
15 J. M. Campos, M. R. Ribeiro, J. P. Lourenço and A. Fernandes, *J. Mol. Catal. A: Chem.*, 2007, **277**, 93.
16 J. M. Campos, J. P. Lourenço, H. Cramail and M. R. Ribeiro, *Prog. Polym. Sci.*, 2012, **37**, 1764.
17 P. A. Zapata, R. Quijada, I. Lieberwirth and H. Palza, *Appl. Catal. A: Gen.*, 2011, **407**, 181.
18 (a) X. Duan and D. G. Evans, *Layered double hydroxides*, Springer Verlag, 2006; (b) V. Rives, *Layered double hydroxides: present and future*, Nova Science Publishers, 2001; (c) F. Cavani, F. Trifiro and A. Vaccari, *Catal. Today*, 1991, **11**, 173. (d) Q. Wang and D. O'Hare, *Chem. Rev.*, 2012, **112**, 4124.
19 Q. Wang and D. O'Hare, *Chem. Commun.*, 2013, **49**, 6301.
20 Q. Wang, J. Undrell, Y. Gao, G. Cai, J.-C. Buffet, C. A. Wilkie and D. O'Hare, *Macromolecules*, 2013, **46**, 6145.
21 (a) C. Chen, M. Yang, Q. Wang, J.-C. Buffet and D. O'Hare, *J. Mater. Chem. A.*, 2014, **2**, 15102. (b) M. Yang, O. McDermott, J.-C. Buffet and D. O'Hare, *RSC Adv.*, 2014, **4**, 51676. (c) C. Chen, A. Wangriya, J.-C. Buffet and D. O'Hare, *Dalton Trans.*, 2015, **44**, 16392.
22 J.-C. Buffet, N. Wanna, T. A. Q. Arnold, E. K. Gibson, P. P. Wells, Q. Wang, J. Tantirungrotechain and D. O'Hare, *Chem. Mater.*, 2015, **27**, 1495
23 J.-C. Buffet, Z. R. Turner, R. T. Cooper and D. O'Hare, *Polym. Chem.*, 2015, **6**, 2493.
24 F. M. Alias, S. Barlow, J. S. Tudor, D. O'Hare, R. T. Perry, J. M. Nelson and I. Manners, *J. Organomet. Chem.*, 1997, **528**, 47.
25 W. A. Herrmann, J. Rohrmann, E. Herdtweck, W. Spaleck and A. Winter, *Angew. Chem. Int. Ed.*, 1989, **28**, 1511.
26 A. V. Churakov, J. A. K. Howard and A. Z. Voskoboynikov, *J. Organomet. Chem.*, 2005, **690**, 1067.
27 T. Repo, M. Klinga, I. Mutikainen, Y. Su, M. Leskelä, M. Polamo, M. N. Homsi, F. K. H. Kuske, M. Haugg, N. Trabesinger-Rüf and E. G. Weinhold, *Acta Chem. Scand.*, 1996, **50**, 1116.
28 A. D. Becke *J. Chem. Phys.*, 1986, **84**, 4524.
29 A. D. Becke *J. Chem. Phys.*, 1993, **98**, 5648.
30 C. Lee, W. Yang, W. and R. G. Parr, *Phys. Rev. B*, 1988, **37**, 785.
31 A. D. Becke, *Phys. Rev. A*, 1988, **38**, 3098.
32 J. Perdew, *Phys. Rev. B,* 1986, **33**, 8822.
33 L. M. Engelhardt, R. I. Papasergio, C. L. Raston and A. H. White, *Organometallics,* 1984, **3**, 18.
34 F. Silveira, M. Alves, F. C. Stedile, S. B. Pergher, and J. H. Z. dos Santos, *J. Mol. Catal. A Chem.*, 2010, **315**, 213.
35 R. Guimarães, F. C. Stedile, and J. H. Z. dos Santos, *J. Mol. Catal. A Chem.*, 2003, **206**, 353.
36 W. Kaminsky, *J. Chem. Soc. Dalton Trans.*, 1998, 1413
37 W. Kaminsky, R. Engehausen, K. Zoumis, W. Spaleck and J. Rohrmann, *Makromol. Chem.*, 1992, **193**, 1643.
38 M. Eskelinen and J. V. Seppälä, *Eur. Polym. J.*, 1996, **32**, 331.
39 J. R. Severn, J. C. Chadwick, R. Duchateau, and N. Friederichs, *Chem. Rev.*, 2005, **105**, 4073.
40 T. A. Q. Arnold, J.-C. Buffet, Z. R. Turner and D. O'Hare, *J. Organomet. Chem.*, 2015, **792**, 55.
41 L. D'Agnillo, J. B. P. Soares and A. Penlidis, *Macromol. Chem. Phys.*, 1998, **199**, 955
42 B. Rieger and C. Janiak, *Angew. Makromol. Chemie*, 1994, **215**, 35.

43 D.-H. Lee, S.-Y. Shin and D.-H. Lee, *Macromol. Symp.,* 1995, **97**, 195.
44 J. Cosier and A. M. Glazer, *J. Appl. Crystallogr.*, 1986, **19**, 105.
45 Z. Otwinowski and W. Minor, *Methods Enzymol.*, 1997, **276**, 307.
46 R. H. Blessing, *Acta Crystallogr., Sect. A: Fundam. Crystallogr.*, 1995, **A51**, 33.
47 G. M. Sheldrick, Acta Crystallogr., Sect. A: Found. Crystallogr., 2008, 64, 112-122.
48 L. Palatinus and G. Chapuis, *J. Appl. Crystallogr.*, 2007, **40**, 786.
49 L. J. Farrugia, J. Appl. Crystallogr., 1999, 32, 837-838.
50 CrysAlisPRO, Oxford Diffraction/Agilent Technologies UK Ltd, Yarnton, England.
51 P. W. Betteridge, J. R. Carruthers, R. I. Cooper, K. Prout and D. J. Watkin, *J. Appl. Crystallogr.*, 2003, **36**, 1487
52 R. I. Cooper, A. L. Thompson and D. J. Watkin, *J. Appl. Crystallogr.*, 2010, **43**, 1100.